Journal of Materials Chemistry

Cite this: J. Mater. Chem., 2011, 21, 13241

www.rsc.org/materials

PAPER

Graphene buffered galvanic synthesis of graphene–metal hybrids†

Zhen Li,[a] Peng Zhang,[a] Kunlin Wang,[a] Zhiping Xu,[b] Jinquan Wei,[a] Lili Fan,[a] Dehai Wu[a] and Hongwei Zhu*[ab]

Received 19th April 2011, Accepted 16th June 2011
DOI: 10.1039/c1jm11695a

We report an *in situ* synthesis of graphene–metal hybrids using graphene as the buffer layer by a substrate-induced galvanic reaction. Ag nanoplates are obtained with the template effect of graphene, and their morphologies are tailored by light mediation. Our result suggests that defect sites or open edges of graphene favor binding with Ag atoms. The graphene–Ag hybrids have been used as Raman enhanced substrates for dye detection. The facile method for synthesis of graphene–metal hybrids opens up opportunities for the future development of optical, electronic and catalytic materials based on graphene and metals.

Introduction

Graphene, a monolayer of carbon atoms with a honeycomb lattice structure, has many intriguing properties with great application potential.[1,2] This novel flat carbon geometry provides new opportunities for designing two-dimensional (2D) hybrid assemblies. For example, graphene is an ideal atomic template for van der Waals epitaxy of topological insulators,[3–5] π-assembly of aromatic organic molecules[6] and monodispersion of nanocrystals.[7] Its high conductance, chemical stability and large surface area make graphene a novel platform for nanocomposites.[8] Graphene films decorated with quantum dots,[9,10] nanoparticles,[11,12] nanowires,[13–15] nanotubes[16,17] and nanosheets[18,19] have demonstrated superior properties compared to individual constituent components.

Among these novel nanocomposites/hybrids, graphene–metal composites have drawn great attention because of the tunable surface properties of graphene and the prospects for industrial catalytic applications.[20–22] Many metal nanoparticles can be decorated on graphene by the wet-chemistry method[23–26] or metal evaporation.[27] However, some of these methods involve complex multi-step processes or require complicated vacuum equipment. For example, the wet-chemistry methods usually use graphite oxides as the starting materials for good dispersion in solutions to achieve a high yield for large-scale applications. However, in terms of quality and continuity, the reduced graphene oxide is not as good as graphene films obtained by chemical vapor deposition (CVD) or mechanical exfoliation.

As key components of the hybrid structure, graphene and metal nanostructures are both of great interest in many optical and optoelectronic applications. For example, graphene is one of the excellent candidates for laser mode-locking[28] and transparent conductors.[29] By tuning their sizes and geometries, metal nanostructures with different surface plasmon resonances show wide varieties of optical properties.[30,31] However, despite its importance, the graphene–metal nanostructure system has not been well understood.

In this paper, we introduce a rational method using graphene as a buffer layer and template for deposition of inactive metals on graphene films by a substrate-induced galvanic reaction. This method refers to a mechanism similar to a previous report of depositing metal nanoparticle on carbon nanotubes.[32] Our galvanic method offers several advantages, including its simplicity and universality (applicable to all kinds of graphene materials and many metals). Moreover, the geometry of the metallic nanostructures could be tailored by the intrinsic 2D structure of graphene plus additional light illumination applied during metal deposition. With the template effect of graphene and light mediation, Ag nanoplates with varied sizes and morphologies have been grown on graphene, forming a novel Ag-on-graphene hybrid *in situ*. Raman spectroscopy is used for examination of the graphene–Ag coupling. 2D hybrids of graphene–Ag nanoplates are also evaluated as Raman enhanced substrates for dye detection.

Experimental

Synthesis of graphene films

Graphene films were prepared by an atmospheric pressure CVD. Briefly, a piece of 20 μm thick copper foil was heated to 1050 °C in a mixture flow of Ar/H_2 (100/5 mL min^{-1}) in a 1-inch quartz reactor. Methane of 25 mL min^{-1} was then introduced. The growth duration is 5–10 min. The copper foil (with graphene

[a]*Key Laboratory for Advanced Manufacturing by Materials Processing Technology, Department of Mechanical Engineering, Tsinghua University, Beijing, 100084, China. E-mail: hongweizhu@tsinghua.edu.cn*
[b]*Center for Nano and Micro Mechanics, Tsinghua University, Beijing, 100084, P. R. China*

† Electronic supplementary information (ESI) available: Simulation method, SEM and TEM images of graphene–metal hybrids. See DOI: 10.1039/c1jm11695a

grown on top) was pulled out and allowed to cool to room temperature under the protection of Ar.

Deposition of Ag nanoplates

The as-obtained graphene/Cu substrate was immersed in a diluted $AgNO_3$ solution (0.01–1 mM) for 5–20 min for nanoplate deposition. Illumination conditions: 1) faint light from a household fluorescent lamp; 2) simulated solar light (AM1.5) with a power density of 100 mW cm^{-2}, generated from a solar simulator (Newport 91159); 3) laser beams with a power of 100 mW, wavelengths of 473 nm (blue), 532 nm (green), and 635 nm (red). The growth of Ag nanoplates is based on a galvanic replacement reaction between Cu and Ag.

Structural characterizations of Ag nanoplates

The morphology of Ag nanoplates deposited on graphene was directly imaged by scanning electron microscopy (SEM, LEO-1530). For other characterizations, the graphene-Ag hybrid films were first transferred to target substrates (*e.g.* Cu grids, Si wafers) by etching away the copper foil in a mixture solution of 0.5 M HCl and 0.5 M $FeCl_3$. The detail of the transfer process has been described in our previous work.[33] Transmission electron microscopy (TEM, JEM-2010) and atomic force microscopy (AFM, Agilent Picoscan-5100) were employed to characterize the structures of Ag nanoplates.

Raman spectra

Raman spectra were taken by a Raman spectroscope (Renishaw RM-1000) equipped with a 514 nm laser, within a spot diameter of 10 μm. For surface enhanced Raman spectroscopy (SERS) detection of Rhodamine B, the graphene–Ag hybrid film was first transferred to a SiO_2 substrate and soaked in the ethanol solution of Rhodamine B (10^{-6} M) for ~1 h. The sample was then taken out and allowed to dry in a nitrogen flow. Raman spectra were obtained by subtracting the fluorescence background and normalizing the lowest intensity to zero.

Results and discussion

The so-called graphene buffered galvanic reaction is described in Fig. 1a. As the graphene film grown on a reductive substrate (*e.g.* copper) was immersed into an oxidant solution (*e.g.* Ag^+), a substrate-induced galvanic displacement took place. The copper substrate served as the scarified metal, providing electrons for metal deposition when it was dissolved. The graphene film served as a buffer layer, which could shuttle electrons over some distance for metal nucleation and subsequent crystal growth.[34] Ag nanostructures deposited on graphene films showed various morphologies, ranging from dots and hemi-spheres to polygon nanoplates [see SEM images in Fig. 2, 3]. The morphology of these nanostructures depended strongly on the particular growth conditions with varying Ag^+ concentration, illumination and growth duration.

To verify the mechanism of *in situ* metal growth on graphene in the galvanic reaction, a primary battery test was carried out (Fig. 1b). The graphene film was first transferred to a PET film by hot rolling, followed by substrate etching and washing. Then, the

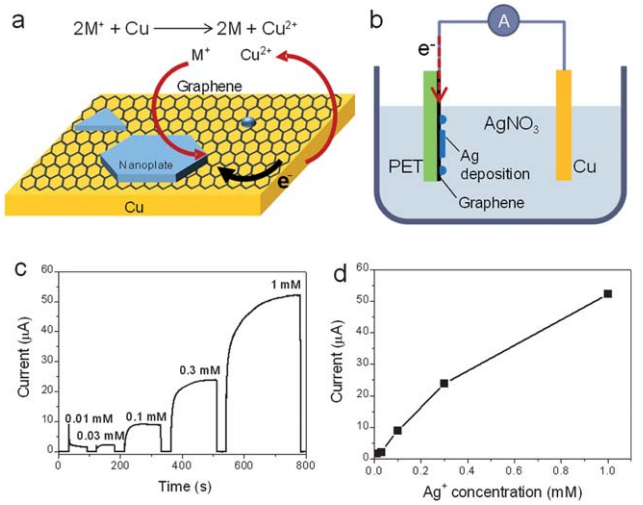

Fig. 1 (a) A schematic of *in situ* galvanic synthesis of graphene–Ag hybrids. (b) Schematic of a primary battery made from graphene/PET and copper. (c) Output current of the primary battery. (d) Correlation between the output current and Ag^+ concentration.

graphene/PET film (as the cathode) and a clean copper foil (as the anode) were immersed into a dilute $AgNO_3$ solution, facing each other with a spacing of ~1 cm. During Ag deposition, the output current was equivalent to electron transfer rate from copper to graphene. As shown in Fig. 1c, d, higher concentration Ag^+ yielded a larger current output, resulting in a faster Ag deposition rate on graphene. Consequently, Ag nanostructures with various morphologies could be obtained on graphene (Figure S1†). The result provides further evidence for the galvanic reaction proposed in Fig. 1a.

The substrate enhanced galvanic reaction takes advantage of the dual role of copper, which acts as both the CVD substrate for

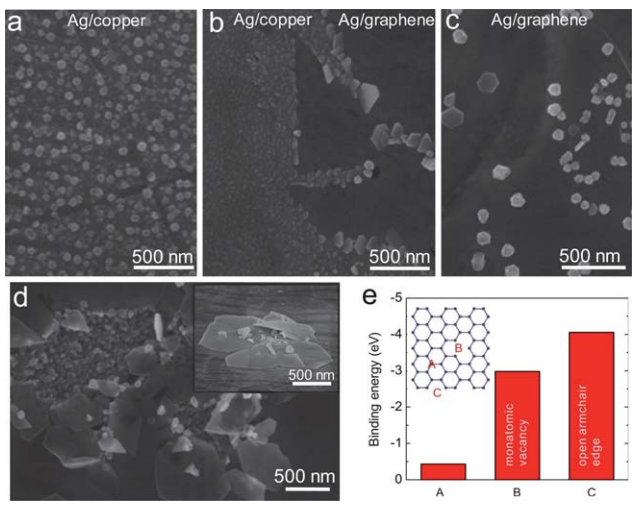

Fig. 2 SEM images of Ag nanostructures. (a) Nanoparticles deposited on bare copper surface. (b) Morphology transition near the boundary between copper (left) and graphene (right). (c) Nanoplates deposited on graphene. (d) Nanoplates grown over cracks on graphene. Inset: tilt-view of nanoplates on graphene. (e) Binding sites and energies of an Ag atom on a graphene sheet. A: on the top of the basal plane, B: on the top of a monatomic vacancy site, C: at the armchair edge.

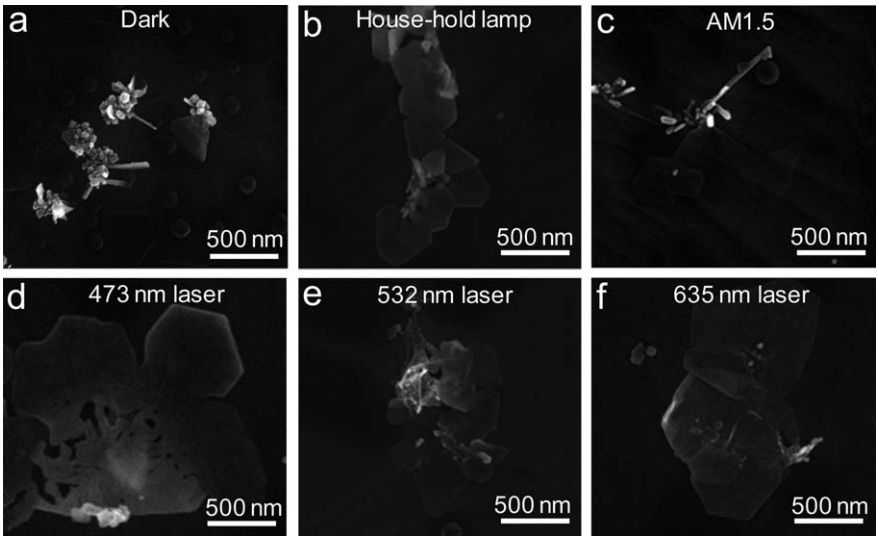

Fig. 3 SEM images of light-induced Ag nanoplates obtained under (a) dark, (b) faint fluorescent light, (c) simulated solar light (AM1.5), (d) 473 nm blue laser, (e) 532 nm green laser, (f) 635 nm red laser.

graphene growth and the scarified metal for Ag reduction. Compared to other synthesis of graphene–metal hybrids/composites (using chemical derived graphene as the starting material), the substrate-induced metal deposition is a one-step process without any damage to the intrinsic structure of graphene. The continuous and highly conductive CVD-synthesized graphene film is more suitable for thin film applications, such as optical transparent electrodes and flexible electronics. The galvanic displacement process avoids chemical modification of graphene films, thus retaining the intriguing properties of graphene, such as high carrier mobility and conductance.

It is further revealed that graphene plays important roles during the galvanic synthesis. Ag nanostructures deposited on sole copper and on graphene/copper through galvanic displacement show great differences in morphology. A control experiment was conducted to elucidate the influence of the presence of graphene on the morphology of Ag deposition. Part of the graphene film on the copper foil was wiped out to expose the copper surface underneath. The copper foil with partially removed graphene film was immersed in a 0.1 mM $AgNO_3$ solution for Ag deposition under the illumination of a 635 nm laser (with power of 100 mW), an optimal illumination condition for depositing nanoplates of the largest size. On bare copper surfaces, a straightforward galvanic replacement took place between Cu and Ag^+, resulting in closely packed nanoparticles of small size (Fig. 2a). In contrast, with the presence of graphene, the galvanic reaction formed flat, sparsely distributed Ag nanoplates of larger sizes (Fig. 2b, c). These nanoplates have diverse shapes of irregular polygons with relatively smooth surfaces, clearly showing the difference in morphology with the nanoparticles deposited on the bare copper surface.

The influence of graphene on Ag deposition could be attributed to two factors. First, the nucleation rate of Ag is much faster on the copper surface than on the smooth and chemically inert graphene surface. Nucleation sites evenly distributed over the copper surface limit the sizes of individual Ag particles, resulting in ultrafine nanoparticles. Meanwhile, Ag prefers to nucleate on graphene at the imperfections, *e.g.* surface wrinkles, defects and cracks (see Fig. 2d). After the initial nucleation, Ag atoms tend to accumulate on the nuclei to form larger sized structures, *e.g.* the nanoplate. The tendency of Ag nucleation at the imperfections can be used as an indicator to detect surface defects on graphene, which are usually difficult to distinguish by SEM. Well controlled Ag deposition is expected to be an innovative way for graphene quality and continuity evaluation (Figure S2†). First-principles calculations are performed to obtain the binding energy (E_b) between one silver atom and pristine or defected graphene sheets (see ESI for details†). Three binding sites are considered in our calculations: the position on the hexagon of a pristine graphene (A), a pristine graphene with a monovacancy (B) and at the armchair edge of a graphene sheet (C). The result is summarized in Fig. 2e. For site (A), the silver atom sits on the carbon atom with an interatomic distance of 0.243 nm. The silver atom features an electronic configuration of [Kr] $4d^{10}5s^1$, thus will form a covalent binding with the carbon atoms with dangling bonds, such as those at defective sites (B) or edges (C). The bond length between silver and carbon atoms is 0.21 nm for site C, which is close to the sum of the covalent radii of silver and carbon, indicating a covalent bonding nature. The result suggests that the defected sites or open edges of graphene favor binding with Ag atoms.

Second, providing that the copper surface is fully covered by graphene, the galvanic reaction, including copper oxidation and Ag reduction will take place at different locations. Electrons for Ag^+ reduction could be shuttled by the graphene film over a distance. The flat platform of graphene acts as a template, guiding the growth of the quasi 2D nanoplate. A previous study showed that naturally grown Ag by reduction of Ag^+ usually assembled into dendrite-like structures.[35] Under surfactant protection, a preferred growth of the Ag(111) plane could be realized.[36] Different to the graphene templated synthesis of nanomaterials in other material systems,[6,7,37,38] our *in situ* deposition of Ag nanoplates on graphene provides clean surfaces without any surfactant capping and organic contaminations. This may pave the way for further investigation on surface plasmonics of Ag nanoplates and graphene/Ag coupling.

The kinetics of the graphene-guided galvanic growth of Ag nanoplates was further investigated by varying the Ag^+ concentration for selective deposition. When the concentration of Ag^+ was as high as 10 mM, the Ag nucleation on graphene was not limited to any specific location, and the resulting materials are uniformly distributed spherical nanoparticles rather than nanoplates (Figure S3a†). When the concentration of Ag^+ was as low as 0.01 mM, the nucleation could be only observed at wrinkles and cracks on the graphene film. Without a sufficient amount of Ag^+ for nanoplate growth, Ag deposition generated small dots with some of them growing into triangle disks (Figure S3b†). The suitable concentration for Ag nanoplate deposition is 0.05–1 mM based on our experimental results.

Another important aspect of our work is that light illumination shows strong influence on the morphology of Ag nanoplates. Fig. 3a–f show Ag nanoplates deposited on graphene films under different illumination conditions. Ag tends to aggregate into clusters in the dark to form relatively small nanoparticles. In contrast, under illuminations of a variety of light sources, including faint room light, intensive simulated solar light and laser beams, the resulting flat nanoplates show diverse morphologies with different sizes and shapes. The faint light from a standard household fluorescent lamp produced a large amount of triangular and truncated triangular nanoplates with uniform dimensions (Fig. 3b). Under the simulated solar light (AM1.5) with a power density of 100 mW cm^{-2}, Ag tended to grow into a stripe-like shape from the center, then expanded to form a leaf-like flat plate (Fig. 3c). When irradiated by single wavelength laser beams, Ag nanoplates became larger in size and showed shapes of fused or overlapping polygons. Specifically, Ag nanoplates obtained under blue laser (473 nm) irradiation were thicker with much more irregular profiles compared to those from the other two lasers. The green laser (532 nm) produced a high ratio of truncated triangle shaped nanoplates. Larger and thinner overlapping hexagonal nanoplates were obtained with the red laser (635 nm) irradiation. To rule out the heating effect during the illumination, which might also contribute to the morphology deviations of Ag nanoplates, control experiments were carried out in $AgNO_3$ solutions in dark with temperatures of ~50 °C maintained in a warm water bath. Ag thus deposited showed obvious particle-like structure, which differed from the above-mentioned photo-induced nanoplate deposition.

Considering the fact that Ag nanoplates grow larger in light than in the dark during same the growth durations (Fig. 3a–f), it is concluded that light promotes the growth of nanoplates. It has been known that light mediates the morphology and size of Ag colloids. Upon illumination, nanoplates and nanoprisms of Ag show higher yields over spherical nanoparticles.[39] The edge length of nanoplates could be tuned by the wavelength of irradiation.[40] The mechanism of our light mediated synthesis of Ag nanoplates is thought to be photo-induced growth or aggregation. In detail, the photo-induced growth refers to the catalytic photo-oxidation of certain reductants for the reduction of Ag^+. In the case of the graphene buffered nanoplate growth, as-deposited Ag and the copper substrate (with different work functions) act as asymmetrical metal contacts with graphene. Photo-induced electrons inject into metal contacts. The electron flow from graphene to the lower work function metal (Ag) is greater than that for the higher work function metal (Cu). The net photocurrent promotes the reduction of Ag^+. The anisotropic growth of nanoplates relies on the intrinsic characteristics of Ag seeds. The photo-induced aggregation mechanism is based on light-induced ripening and fusion of small spherical seeds and smaller triangles into larger nanoplates driven by localized surface plasmon resonances,[39] mainly contributing to the shape variation of nanoplates under different wavelength illuminations.

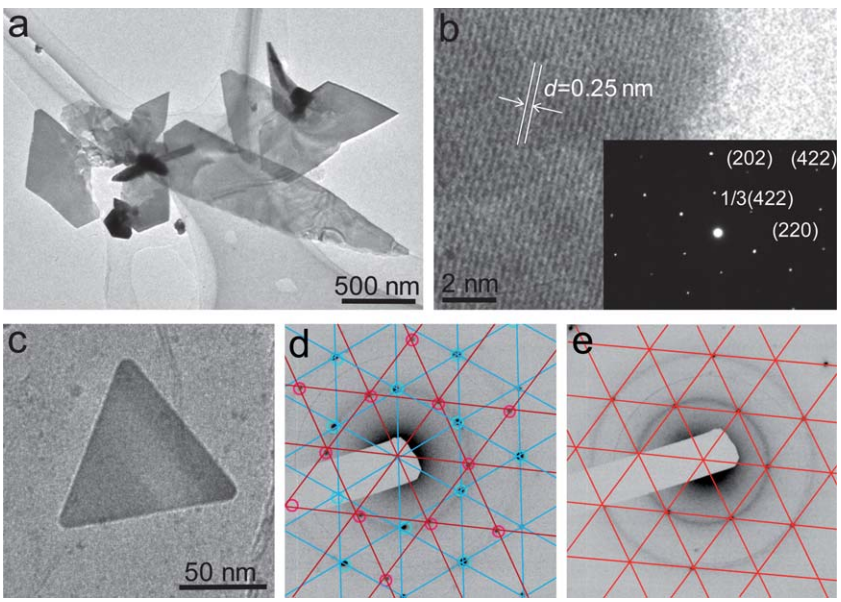

Fig. 4 TEM images and SAED patterns of Ag nanoplates. (a–c) TEM images. The inset of (b) shows the SAED pattern with plane index. (d) Superimposed SAED pattern with blue grids for Ag *fcc* lattice and red grids for graphene hexagonal lattice. (e) SAED pattern taken at a nearby location from sole graphene for identification of the graphene lattice in the superimposed pattern.

Fig. 4 shows the TEM characterizations of Ag nanoplates. High resolution TEM image (Fig. 4b) of a typical nanoplate shows parallel fringes with a spacing of 0.25 nm, corresponding to (1/3){422} of the face center cubic (*fcc*) Ag lattice. The selected area electron diffraction (SAED) pattern (inset of Fig. 4b) further confirms its *fcc* structure. The inner-most six bright spots with 6-fold symmetry are indexed as (1/3){422}. Stacking faults of {111} planes bring out the (1/3){422} reflection, which is normally forbidden in *fcc* lattice.[40] The six spots on the second ring of the pattern correspond to {220} planes along the <111> orientation, indicating that the {111} plane is parallel to the nanoplate surface. Figure S4† shows the superimposed diffraction patterns of Ag (blue spots) and graphene (red spots). Diffraction spots of Ag are distinguished by taking diffraction from the nearby graphene film. The identification of Ag and graphene spots is further realized by comparing their lattice constants. Mismatch angles are identified in the superimposed diffraction patterns, ranging from 15.0° to 22.5°. The misalignment and random angles between two sets of spots reveal that the galvanic deposition of Ag on graphene is not based on the well-known epitaxial growth.

The graphene/Ag interaction is further probed by Raman spectroscopy. As shown in Fig. 5a, the Raman spectra of graphene–Ag hybrid films obtained under different illumination conditions are compared. The spectra reveal three typical groups of bands: the G band of 1580–1600 cm^{-1} related to the tangential stretching mode of sp^2 carbon, the D band of 1350–1400 cm^{-1} related to defects of the graphene lattice, and the 2D band of 2600–2800 cm^{-1}, which is sensitive to the electronic and/or phonon structures of graphene.[41] The pristine graphene shows a typical spectrum of monolayer feature with a I_{2D}/I_G ratio of ~2.5. The weak D band indicates that few defects are present in the pristine graphene. After deposition of Ag nanoplates, Raman spectra show several new features: i) significant enhancement of D band is observed for all samples; ii) enhanced G band except for the red laser mediated Ag nanoplates, with enhancements of 220% and 520% for nanoplates grown under green laser and the simulated solar light; iii) suppressed 2D band with I_{2D}/I_G ratios of less than 0.2. Based on the growth mechanism of nanoplates proposed above, Ag nanoplates are more likely to assemble around the defect sites on graphene. With collected Raman scattering from the defect sites enhanced by Ag nanoplates, the weight of defects in the resulting spectrum is higher. Therefore, the spectra show the obvious increase of the D band intensity. SERS of graphene decorated with metal nanoparticles (Au, Pt) has been reported,[42] which is mainly attributed to charge transfer between metal and graphene. This is also consistent with the observed blue shifts of the G band, as shown in the inset of Fig. 5a. It was also reported that with electron or hole doping, Raman spectra of graphene show behaviors, such as stiffening of the G band (blue shift) and suppressing of the 2D band.[43] The quasi 2D structure of Ag nanoplates will introduce a stronger metal/graphene coupling than spherical nanoparticles.[44] Therefore, the charge transferring process between Ag nanoplates and graphene greatly contribute to the Raman variations. However, the detailed influences of the size and morphology of Ag nanoplates on SERS of graphene need further investigation.

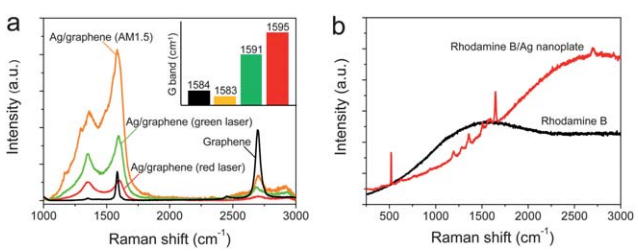

Fig. 5 (a) The Raman spectra of light-induced graphene–Ag hybrids. (b) SERS of Rhodamine B.

Beside Ag nanostructures, monolayer graphene can serve as a Raman enhanced substrates as well.[45,46] The graphene–Ag hybrid film is tested as a SERS substrate for detection of Rhodamine B dye. As shown in Fig. 5b, the Raman scattering of Rhodamine B absorbed on SiO_2 shows only a fluorescence background without any detectable Raman peaks. After applying the same trace amount of dye to the graphene/Ag film, the Raman spectrum shows detailed peaks of the dye. It is so demonstrated that the hybrid film is an effective substrate for SERS.

Conclusions

We have developed an *in situ* graphene buffered synthesis of graphene–Ag hybrids using the galvanic displacement of metals. With the template effect of 2D graphene, Ag nanoplates are obtained and their morphologies can be tailored by illumination, which further influences the Ag/graphene coupling. The graphene–Ag hybrid films have been used as Raman enhanced substrates for dye detection. The graphene buffered deposition is applicable to all kinds of graphene materials (see Figure S5†) and can be extended to many metals to prepare various metal/metal oxide nanostructures (see Figure S6†). The facile method for the synthesis of graphene–metal hybrids opens opportunities for the future development of optical, electronic and catalytic materials based on graphene and metals.

Acknowledgements

This work was supported by National Science Foundation of China (#50972067), Tsinghua University Initiative Scientific Research Program (#2009THZ02123) and Research Fund for Doctoral Program of Ministry of Education of China (#20090002120019).

References

1 K. S. Novoselov, A. K. Geim, S. V. Morozov, D. Jiang, Y. Zhang, S. V. Dubonos, I. V. Grigorieva and A. A. Firsov, Electric Field Effect in Atomically Thin Carbon Films, *Science*, 2004, **306**, 666–669.
2 A. K. Geim and K. S. Novoselov, The Rise of Graphene, *Nat. Mater.*, 2007, **6**, 183–191.
3 W. H. Dang, H. L. Peng, H. Li, P. Wang and Z. F. Liu, Epitaxial Heterostructures of Ultrathin Topological Insulator Nanoplate and Graphene, *Nano Lett.*, 2010, **10**, 2870–2876.
4 C. L. Song, Y. L. Wang, Y. P. Jiang, Y. Zhang, C. Z. Chang, L. L. Wang, K. He, X. Chen, J. F. Jia, Y. Y. Wang, Z. Fang, X. Dai, X. C. Xie, X. L. Qi, S. C. Zhang, Q. K. Xue and X. C. Ma, Topological Insulator Bi_2Se_3 Thin Films Grown on Double-layer Graphene by Molecular Beam Epitaxy, *Appl. Phys. Lett.*, 2010, **97**, 143118.

5 X. Chen, X. C. Ma, K. He, J. F. Jia and Q. K. Xue, Molecular Beam Epitaxial Growth of Topological Insulators, *Adv. Mater.*, 2011, **23**, 1162–1165.
6 S. Wang, B. M. Goh, K. K. Manga, Q. L. Bao, P. Yang and K. P. Loh, Graphene as Atomic Template and Structural Scaffold in the Synthesis of Graphene-Organic Hybrid Wire with Photovoltaic Properties, *ACS Nano*, 2010, **4**, 6180–6186.
7 Y. Pan, M. Gao, L. Huang, F. Liu and H. J. Gao, Directed Self-assembly of Monodispersed Platinum Nanoclusters on Graphene Moire Template, *Appl. Phys. Lett.*, 2009, **95**, 093106.
8 P. V. Kamat, Graphene-Based Nanoarchitectures. Anchoring Semiconductor and Metal Nanoparticles on a Two-Dimensional Carbon Support, *J. Phys. Chem. Lett.*, 2010, **1**, 520–527.
9 X. M. Geng, L. Niu, Z. Y. Xing, R. S. Song, G. T. Liu, M. T. Sun, G. S. Cheng, H. J. Zhong, Z. H. Liu, Z. J. Zhang, L. F. Sun, H. X. Xu, L. Lu and L. W. Liu, Aqueous-Processable Noncovalent Chemically Converted Graphene-Quantum Dot Composites for Flexible and Transparent Optoelectronic Films, *Adv. Mater.*, 2010, **22**, 638.
10 C. X. Guo, H. B. Yang, Z. M. Sheng, Z. S. Lu, Q. L. Song and C. M. Li, Layered Graphene/Quantum Dots for Photovoltaic Devices, *Angew. Chem., Int. Ed.*, 2010, **49**, 3014–3017.
11 S. M. Paek, E. Yoo and I. Honma, Enhanced Cyclic Performance and Lithium Storage Capacity of SnO2/Graphene Nanoporous Electrodes with Three-Dimensionally Delaminated Flexible Structure, *Nano Lett.*, 2009, **9**, 72–75.
12 H. Zhang, X. J. Lv, Y. M. Li, Y. Wang and J. H. Li, P25-Graphene Composite as a High Performance Photocatalyst, *ACS Nano*, 2010, **4**, 380–386.
13 Z. S. Wu, W. C. Ren, D. W. Wang, F. Li, B. L. Liu and H. M. Cheng, High-Energy MnO_2 Nanowire/Graphene and Graphene Asymmetric Electrochemical Capacitors, *ACS Nano*, 2010, **4**, 5835–5842.
14 S. Biswas and L. T. Drzal, Multi Layered Nanoarchitecture of Graphene Nanosheets and Polypyrrole Nanowires for High Performance Supercapacitor Electrodes, *Chem. Mater.*, 2010, **22**, 5667–5671.
15 D. Choi, M. Y. Choi, W. M. Choi, H. J. Shin, H. K. Park, J. S. Seo, J. Park, S. M. Yoon, S. J. Chae, Y. H. Lee, S. W. Kim, J. Y. Choi, S. Y. Lee and J. M. Kim, Fully Rollable Transparent Nanogenerators Based on Graphene Electrodes, *Adv. Mater.*, 2010, **22**, 2187.
16 V. C. Tung, L. M. Chen, M. J. Allen, J. K. Wassei, K. Nelson, R. B. Kaner and Y. Yang, Low-Temperature Solution Processing of Graphene-Carbon Nanotube Hybrid Materials for High-Performance Transparent Conductors, *Nano Lett.*, 2009, **9**, 1949–1955.
17 D. H. Lee, J. E. Kim, T. H. Han, J. W. Hwang, S. Jeon, S. Y. Choi, S. H. Hong, W. J. Lee, R. S. Ruoff and S. O. Kim, Versatile Carbon Hybrid Films Composed of Vertical Carbon Nanotubes Grown on Mechanically Compliant Graphene Films, *Adv. Mater.*, 2010, **22**, 1247.
18 H. L. Wang, H. S. Casalongue, Y. Y. Liang and H. J. Dai, $Ni(OH)_2$ Nanoplates Grown on Graphene as Advanced Electrochemical Pseudocapacitor Materials, *J. Am. Chem. Soc.*, 2010, **132**, 7472–7477.
19 K. K. Manga, Y. Zhou, Y. L. Yan and K. P. Loh, Multilayer Hybrid Films Consisting of Alternating Graphene and Titania Nanosheets with Ultrafast Electron Transfer and Photoconversion Properties, *Adv. Funct. Mater.*, 2009, **19**, 3638–3643.
20 I. Gierz, C. Riedl, U. Starke, C. R. Ast and K. Kern, Atomic Hole Doping of Graphene, *Nano Lett.*, 2008, **8**, 4603–4607.
21 C. Xu, X. Wang and J. W. Zhu, Graphene-Metal Particle Nanocomposites, *J. Phys. Chem. C*, 2008, **112**, 19841–19845.
22 E. Yoo, T. Okata, T. Akita, M. Kohyama, J. Nakamura and I. Honma, Enhanced Electrocatalytic Activity of Pt Subnanoclusters on Graphene Nanosheet Surface, *Nano Lett.*, 2009, **9**, 2255–2259.
23 X. Z. Zhou, X. Huang, X. Y. Qi, S. X. Wu, C. Xue, F. Boey, Q. Y. Yan, P. Chen and H. Zhang, In Situ Synthesis of Metal Nanoparticles on Single-Layer Graphene Oxide and Reduced Graphene Oxide Surfaces, *J. Phys. Chem. C*, 2009, **113**, 10842–10846.
24 R. Hao, W. Qian, L. H. Zhang and Y. L. Hou, Aqueous Dispersions of Tcnq-Anion-Stabilized Graphene Sheets, *Chem. Commun.*, 2008, 6576–6578.
25 W. Qian, R. Hao, Y. L. Hou, Y. Tian, C. M. Shen, H. J. Gao and X. L. Liang, Solvothermal-Assisted Exfoliation Process to Produce Graphene with High Yield and High Quality, *Nano Res.*, 2009, **2**, 706–712.
26 X. Cui, C. Z. Zhang, R. Hao and Y. L. Hou, Liquid-Phase Exfoliation, Functionalization and Applications of Graphene, *Nanoscale*, 2011, **3**, 2118–2126.
27 L. T. Qu and L. M. Dai, Substrate-Enhanced Electroless Deposition of Metal Nanoparticles on Carbon Nanotubes, *J. Am. Chem. Soc.*, 2005, **127**, 10806–10807.
28 Q. L. Bao, H. Zhang, Y. Wang, Z. H. Ni, Y. L. Yan, Z. X. Shen, K. P. Loh and D. Y. Tang, Atomic-Layer Graphene as a Saturable Absorber for Ultrafast Pulsed Lasers, *Adv. Funct. Mater.*, 2009, **19**, 3077–3083.
29 S. Bae, H. Kim, Y. Lee, X. F. Xu, J. S. Park, Y. Zheng, J. Balakrishnan, T. Lei, H. R. Kim, Y. I. Song, Y. J. Kim, K. S. Kim, B. Ozyilmaz, J. H. Ahn, B. H. Hong and S. Iijima, Roll-to-Roll Production of 30-Inch Graphene Films for Transparent Electrodes, *Nat. Nanotechnol.*, 2010, **5**, 574–578.
30 I. Pastoriza-Santos and L. M. Liz-Marzan, Colloidal Silver Nanoplates. State of the Art and Future Challenges, *J. Mater. Chem.*, 2008, **18**, 1724–1737.
31 Q. Zhang, Y. X. Hu, S. R. Guo, J. Goebl and Y. D. Yin, Seeded Growth of Uniform Ag Nanoplates with High Aspect Ratio and Widely Tunable Surface Plasmon Bands, *Nano Lett.*, 2010, **10**, 5037–5042.
32 X. Li, C. Li, H. Zhu, K. Wang, J. Wei, X. Li, E. Xu, Z. Li, S. Luo, Y. Lei and D. Wu, Hybrid Thin Films of Graphene Nanowhiskers and Amorphous Carbon as Transparent Conductors, *Chem. Commun.*, 2010, **46**, 3502–3504.
33 I. V. Lightcap, T. H. Kosel and P. V. Kamat, Anchoring Semiconductor and Metal Nanoparticles on a Two-Dimensional Catalyst Mat. Storing and Shuttling Electrons with Reduced Graphene Oxide, *Nano Lett.*, 2010, **10**, 577–583.
34 L. T. Qu and L. M. Dai, Novel Silver Nanostructures from Silver Mirror Reaction on Reactive Substrates, *J. Phys. Chem. B*, 2005, **109**, 13985–13990.
35 S. H. Chen and D. L. Carroll, Synthesis and Characterization of Truncated Triangular Silver Nanoplates, *Nano Lett.*, 2002, **2**, 1003–1007.
36 A. T. N'Diaye, S. Bleikamp, P. J. Feibelman and T. Michely, Two-Dimensional Ir Cluster Lattice on a Graphene Moire On Ir(111), *Phys. Rev. Lett.*, 2006, 97.
37 M. Jahan, Q. L. Bao, J. X. Yang and K. P. Loh, Structure-Directing Role of Graphene in the Synthesis of Metal–Organic Framework Nanowire, *J. Am. Chem. Soc.*, 2010, **132**, 14487–14495.
38 R. C. Jin, Y. W. Cao, C. A. Mirkin, K. L. Kelly, G. C. Schatz and J. G. Zheng, Photoinduced Conversion of Silver Nanospheres to Nanoprisms, *Science*, 2001, **294**, 1901–1903.
39 R. C. Jin, Y. C. Cao, E. C. Hao, G. S. Metraux, G. C. Schatz and C. A. Mirkin, Controlling Anisotropic Nanoparticle Growth through Plasmon Excitation, *Nature*, 2003, **425**, 487–490.
40 V. Germain, J. Li, D. Ingert, Z. L. Wang and M. P. Pileni, Stacking Faults in Formation of Silver Nanodisks, *J. Phys. Chem. B*, 2003, **107**, 8717–8720.
41 M. S. Dresselhaus, A. Jorio, M. Hofmann, G. Dresselhaus and R. Saito, Perspectives on Carbon Nanotubes and Graphene Raman Spectroscopy, *Nano Lett.*, 2010, **10**, 751–758.
42 X. Q. Fu, F. L. Bei, X. Wang, S. O'Brien and J. R. Lombardi, Excitation Profile of Surface-Enhanced Raman Scattering in Graphene-Metal Nanoparticle Based Derivatives, *Nanoscale*, 2010, **2**, 1461–1466.
43 A. Das, S. Pisana, B. Chakraborty, S. Piscanec, S. K. Saha, U. V. Waghmare, K. S. Novoselov, H. R. Krishnamurthy, A. K. Geim, A. C. Ferrari and A. K. Sood, Monitoring Dopants by Raman Scattering in an Electrochemically Top-Gated Graphene Transistor, *Nat. Nanotechnol.*, 2008, **3**, 210–215.
44 K. Jasuja and V. Berry, Implantation and Growth of Dendritic Gold Nanostructures on Graphene Derivatives: Electrical Property Tailoring and Raman Enhancement, *ACS Nano*, 2009, **3**, 2358–2366.
45 X. Ling, L. M. Xie, Y. Fang, H. Xu, H. L. Zhang, J. Kong, M. S. Dresselhaus, J. Zhang and Z. F. Liu, Can Graphene be Used as a Substrate for Raman Enhancement? *Nano Lett.*, 2010, **10**, 553–561.
46 D. E. Charles, D. Aherne, M. Gara, D. M. Ledwith, Y. K. Gun'Ko, J. M. Kelly, W. J. Blau and M. E. Brennan-Fournet, Versatile Solution Phase Triangular Silver Nanoplates for Highly Sensitive Plasmon Resonance Sensing, *ACS Nano*, 2010, **4**, 55–64.

